Proceedings of the 11th International Conference on Computational and Mathematical Methods in Science and Engineering, CMMSE2011
Benidorm, Spain, 26-30 June 2011

Numerical Prediction of Velocity, Pressure and Shear Rate Distributions in Stenosed Channels

Carla S. Fernandes[1], Ricardo P. Dias[2,3] and Rui Lima[3,4]

[1] *Departamento de Matemática, Escola Superior de Tecnologia e Gestão, Instituto Politécnico de Bragança*
[2] *Departamento de Tecnologia Química e Biológica, Escola Superior de Tecnologia e Gestão, Instituto Politécnico de Bragança*
[3] *CEFT – Centro de Estudos de Fenómenos de Transporte, Faculdade de Engenharia da Universidade do Porto*
[4] *Departamento de Tecnologia Mecânica, Escola Superior de Tecnologia e Gestão, Instituto Politécnico de Bragança*

emails: cveiga@ipb.pt, ricardod@ipb.pt, ruimec@ipb.pt

Abstract

Wall shear rates and pressure developed in circulatory system play an important role on the development of some clinical problems such as atherosclerosis and thrombosis. In the present work, blood flow behaviour was numerically studied in simplified domains and several relevant local properties were determined. The stenosis degree was varied in the distinct studied channels and blood rheology was described by three different models – constant viscosity, power-law model and Carreau model. Pressure attains maximum values in the wall of the atheroma and shear rates achieved maximum values in the top of the atheroma. It was also observed that, with the studied flows, the predictions for velocity and shear rate using non-Newtonian models were very similar. This observation can be explained by the magnitude of the obtained shear rates.

Key words: atheroma, velocity, shear rate, pressure, CFD

 ISBN: 978-84-614-6167-7

1. Introduction

Arthrosclerosis means literally "arteries hardening", however it is a generic term that refers to three patterns of vascular diseases which have the hardening and loss of elasticity of the arteries walls as a common factor [1]. The dominant pattern is atherosclerosis, characterized by the formation of atheromas - fibrous plaques that generally exhibit a centre rich in lipids.

The initial lesion of an atheroma formation can trigger due to the turbulence of the flow. Most of the times, the formation of an atheroma is accomplished by a thrombus formation. It is thought that the location of higher pressures and velocities promote the endothelium lesion and hence the formation of a thrombus, which normally conduce to a thromboembolism due to the high speeds and pressures [1].

2. Numerical Simulations

The governative equations for the isothermal laminar incompressible blood flow were solved by the finite-element software POLYFLOW®. Since experimental study of blood flow in the circulatory system is not an easy task, the numerical results can be useful in order to understand the blood behaviour in stenosed arteries/vessels.

In the calculations, blood was considered both Newtonian and non-Newtonian fluid, its rheology being described, in the second case, by the power-law and Carreau models which can be mathematically expressed, respectively, by:

$$\eta = K\dot{\gamma}^{n-1}, \tag{1}$$

$$\eta = \eta_\infty + (\eta_0 - \eta_\infty)\left[1 + (\lambda\dot{\gamma})^2\right]^{(n-1)/2} \tag{2}$$

where η is the apparent viscosity, K the consistency index, n the flow index behaviour, $\dot{\gamma}$ the shear rate, η_0 the viscosity for lower shear rates, η_∞ the viscosity for higher shear rates and λ the natural time. For blood, the values of all these rheological parameters were presented in Tab.1.

Table 1: Rheological properties of blood [2].

Rheological model	η (Pas)	K (Pas^n)	n (-)	λ (s)	η_∞ (Pas)	η_0 (Pas)
Newtonian	0.00345	-	-	-	-	-
Power-law model	-	0.035	0.6	-	-	-
Carreau model	-	-	0.3568	3.313	0.00345	0.056

 ISBN: 978-84-614-6167-7

The simulations were carried out in 3D geometries representing cylindrical stenosed channels, the atheroma being constructed resorting to a semi-sphere, Fig. 1.

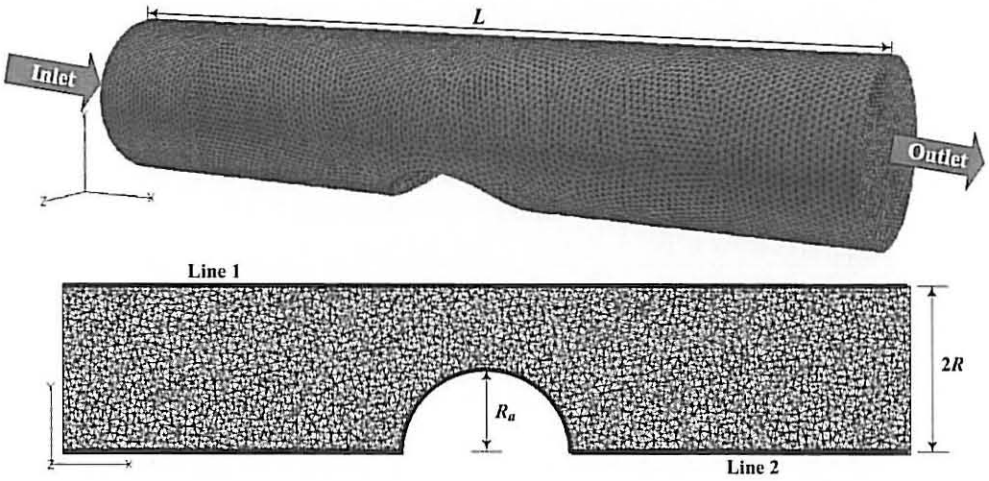

Figure 1: Representation of the computational domain and used mesh.

Three channels presenting different stenosis degrees were studied. All the channels had the same length (L = 30 mm) and radius (R = 3 mm) and the radius of the atheroma varied as presented in Tab. 2. Stenosis degree was defined as the ratio between the diameter of the channel and the radius of the atheroma ($2R/R_a$).

Table 2: Geometrical properties of the studied channels.

Channel	Stenosis degree (%)	Atheroma radius (mm)
C1	20	1.2
C2	30	1.8
C3	50	3.0

The discretization of the geometrical domain was made using an unstructured non-uniform mesh (Fig. 1) and the size of the elements was fixed after a grid independence test in which the size of the elements is successively reduced and the velocity results, obtained with the different meshes, were compared. The results were considered to be independent when a difference below 1% was achieved [3, 4].

The boundary conditions were established in order to reproduce the experimental work developed by Johnston et al. [2] to study the rheology of blood in arteries.

 ISBN: 978-84-614-6167-7

In the inlet ($x = 0$), a constant flow rate - $M_v = 1.27\times10^{-7}$ m^3s^{-1} - was imposed and non-slip at the walls was admitted.

The equations solved were the conservation of mass and momentum equations for laminar incompressible blood flow. Since this is a non-linear problem, it was necessary to use an iterative method to solve the referred equations. In order to evaluate the convergence of this process, a test based on the relative error in the velocity field was performed. For the velocity field, the modification on each node between two consecutive iterations is compared to the value of the velocity at the current iteration. In the present work, the convergence value was set to 10^{-4}, since this value is appropriate for the studied problem [4-8].

In order to verify the reliability and exactness of the computational fluid dynamics (CFD) calculations, two tests were performed: one involving local properties and other with global properties of the flow. First, velocity profiles were compared with the analytical solution for the fully developed flow of a power-law fluid in a cylindrical duct [9]:

$$v(r) = \frac{3n+1}{n}\left[1-\left(\frac{r}{R}\right)^{(n+1)/n}\right]u \tag{3}$$

where u is the average velocity and is given by:

$$u = \frac{M_v}{\pi R^2}. \tag{4}$$

In Fig. 2 it is possible to observe the good agreement between the numerical velocities and Eq. (3) for both Newtonian ($n = 1$) and power-law fluid ($n = 0.6$) (mean deviation of 0.28 % and 1.27% for the Newtonian and power-law fluid, respectively). As expected, the maximum deviations were observed near the wall, since the velocities in this region were close to zero.

 ISBN: 978-84-614-6167-7

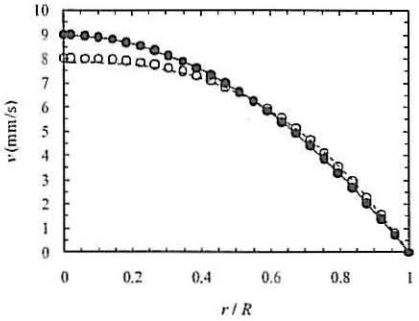

Figure 2: Velocity profiles for fully developed flow in the region before the atheroma in channel C3 for different rheological models. (●) Newtonian; (○) Power-law model; (—) Eq.(3) with $n = 1$; (- - -)Eq.(3) with $n = 0.6$.

To estimate the pressure drop, it is usual to use correlations between Fanning friction factor, f, and Reynolds number, Re. However, when the viscosity of fluid is not constant and difficult to predict, Reynolds number in the relation fRe can be replaced by a generalized Reynolds number, Re_g, the referred relation being:

$$f = a\,\mathrm{Re}_g^{-1} \Leftrightarrow a = f\,\mathrm{Re}_g \tag{5}$$

for fully developed laminar flows. In Eq. (5) a is a constant dependent of the geometry and f is given by:

$$f = \frac{\Delta P D_H}{2L\rho u^2} \tag{6}$$

with ΔP the pressure drop in a channel with length L, ρ the density of the fluid and D_H the hydraulic diameter ($D_H = 2R$ for a cylindrical duct).

The use of Re_g instead of Re allows the calculation of a single friction curve for both Newtonian and non-Newtonian fluids. For flows of power-law fluids in ducts with constant arbitrary section, the following expression for Re_g have been proposed by Delpace and Leuliet [10]:

$$\mathrm{Re}_g = \frac{\rho u^{2-n} D_H^n}{K\left\{(24n+\xi)/\left((24+\xi)n\right)\right\}^n \xi^{n-1}} \tag{7}$$

ξ being a geometrical parameter that assumes the value 8 for cylindrical ducts.

 ISBN: 978-84-614-6167-7

Substituting Eqs. (7) and (6) in Eq. (5), constant a can be expressed as function of rheological and geometrical parameters as follows:

$$a = \frac{D_H^{n+1}\Delta P}{2u^n KL\left\{\left(24n+\xi\right)/\left(\left(24+\xi\right)n\right)\right\}^n \xi^{n-1}}. \tag{8}$$

In order to calculate the constant a for the studied channels, the pressure drop in small cylinders of 1 mm length were used and constant a was estimated resorting to Eq. (8). In the region before the atheroma the average values of a were 16.053 and 15.931 for Newtonian (n = 1 and $K = \eta$ = 0.00345 Pas) and power-law fluid (n = 0.6 and K = 0.035 Pas$^{0.6}$), respectively. Comparing these results with the one predicted analytically (16) it is possible to conclude, once again, that the numerical model used in the present work describes well the studied flow, since the mean deviations were 0.329% and 0.767% for the Newtonian and power-law fluid, respectively.

3. Results and Discussion

In the present work, velocity, pressure and shear rate profiles in stenosed channels were analyzed in order to understand the blood flow when this pathology appears.

In Fig. 3 it is possible to observe that the atheroma leads to a distortion of the velocity profile developed in a cylindrical duct.

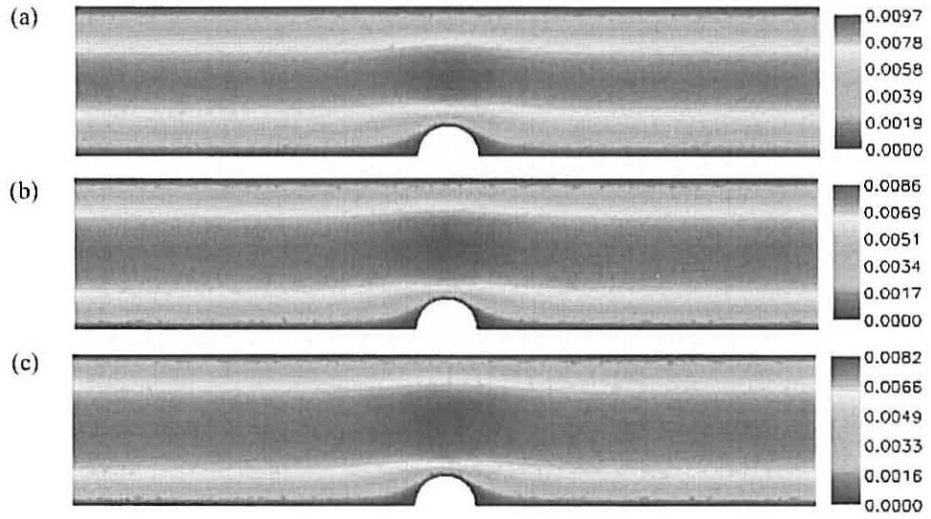

Figure 3: Velocity profiles (ms^{-1}) in the plane z = 0 (see Fig. 1) for channel C1 fluid and distinct rheological models. (a) Newtonian; (b) Power-law model; (c) Carreau model.

 ISBN: 978-84-614-6167-7

The influence of the non-Newtonian behaviour of blood is very small in the velocities developed in the studied channels, since the profiles present very similar aspect and the values of velocity were also very close when considering the different constitutive equations (Fig. 3). However, a lower difference was verified between the velocities obtained for the two non-Newtonian models for the three channels.

Quantitatively, the effect of the atheroma can be evaluated by the increase of the maximum velocity obtained for the stenosed channels compared to the one predicted analytically for a flow of a power-law fluid in a cylindrical duct, which can be determined by (Eq. (3) with $r = 0$):

$$v_{max} = \frac{3n+1}{n+1} u \,. \tag{9}$$

From the values reported in Tab. 3 it is possible to observe that the influence of the atheroma increases with the increase of the stenosis degree, as expected. In the referred table, the values of v_{max} were the ones obtained numerically and I represents the increase of v_{max} due to the presence of the atheroma (v_{max} for the channel without atheroma was calculated by Eq. (9)).

Table 3: Increase of maximum velocity due to the presence of the atheroma.

	C1		C2		C3	
	v_{max} (ms^{-1})	I (%)	v_{max} (ms^{-1})	I (%)	v_{max} (ms^{-1})	I (%)
Newtonian	0.0097	7.977	0.0108	20.2216	0.0151	68.0876
Power-law	0.0086	9.4080	0.0096	22.1299	0.0136	73.017

As observed for the velocity profiles, the shear rate distribution in the different channels and for the different rheological models were qualitatively the same. In Fig. 4 it is possible to observe that shear rate achieve its maximum in the top of the atheroma.

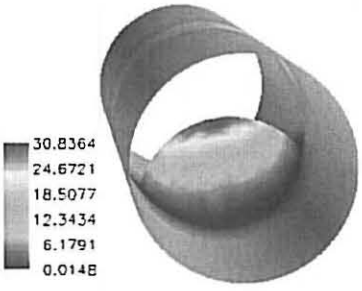

Figure 4: Shear rate in the wall of the channel C3 and Carreau model.

 ISBN: 978-84-614-6167-7

Two lines were considered in a more detailed analysis of shear rate - Lines 1 and 2 represented in Fig.1. This way it was possible to study the impact of the atheroma and rheological properties of the blood in the shear rate along the wall of the channels.

Like observed in the velocity field, the results obtained for the non-Newtonian models where very close (Figs. 5(a) and 6 (a)). The proximity of these results can be explained by the linear behaviour between shear rate and viscosity predicted by the referred models in the range in which this study was performed.

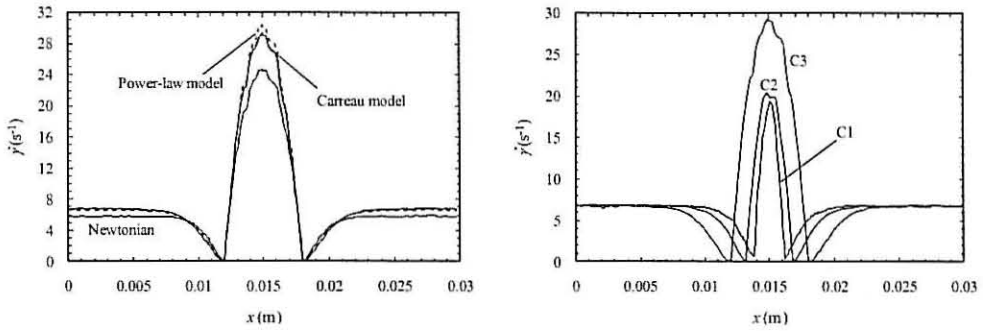

(a) (b)

Figure 5: Shear rate along Line 2 (Fig. 1). (a) Channel C3 and different rheological models. (b) Carreau model and distinct channels.

In Fig. 5(a) the behaviour of the shear rate along Line 2 (Fig. 1) can be clearly observed. Shear rate remains constant in the beginning of the channel for about 4 mm before the atheroma and then decrease until a value close to 0 s^{-1} in the base of the atheroma. Along the wall of the atheroma, shear rate exhibit a parabolic profile the maximum being reached in the top of the atheroma. As expected, the maximum shear rate increase with the increase of stenosis degree, Fig. 5(b).

The impact of the existence of the atheroma along Line 2 is also felt in Line 1 (Fig. 1), as can be observed in Fig. 6.

 ISBN: 978-84-614-6167-7

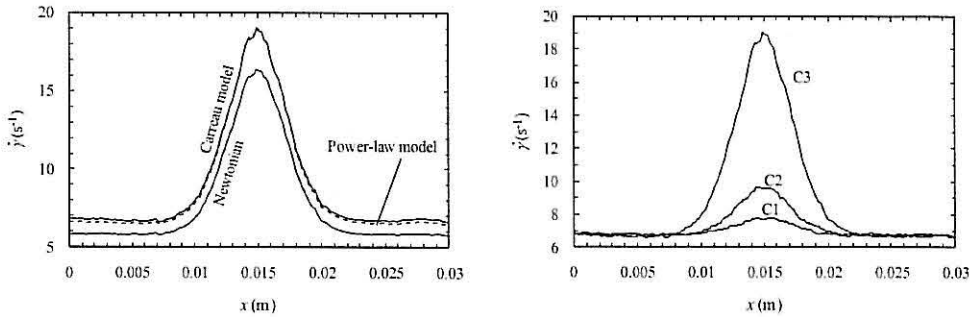

(a) (b)

Figure 6: Shear rate along Line 1 (Fig. 1). (a) Channel C3 for the different rheological models. (b) Carreau model and distinct channels.

Like it was observed for the velocity and shear rate profiles, the pressure fields were qualitatively the same for the distinct channels and rheological models, Fig 7.

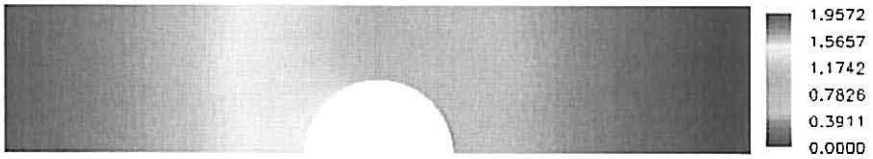

Figure 7: Pressure distribution (Pa) in the plane $z = 0$ for channel C3 and Carreau model.

The pressure profile along Line 2 (Fig. 1) is dependent of the used rheological model and the pressure drop along the atheroma is much lower when the Newtonian behaviour is considered (Fig. 8(a)).

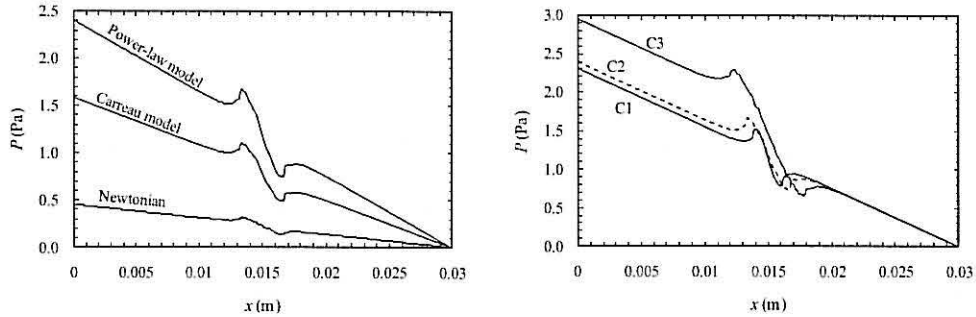

(a) (b)

Figure 8: Pressure along Line 2 (Fig. 1). (a) Channel C2 and distinct rheological models. (b) Power-law model and distinct channels.

 ISBN: 978-84-614-6167-7

In Figs. 8(a) and (b) it can also be observed that the pressure reaches a maximum in the wall of the atheroma.

In the opposite side of the base of the atheroma, Line 1 (Fig.1), the presence of this obstruction is also felt, as can be observed in Fig. 9. Since the influence of the atheroma is much lower along the referred line, the pressure for Newtonian fluid exhibits almost a linear behaviour, as the one existent in a cylindrical duct.

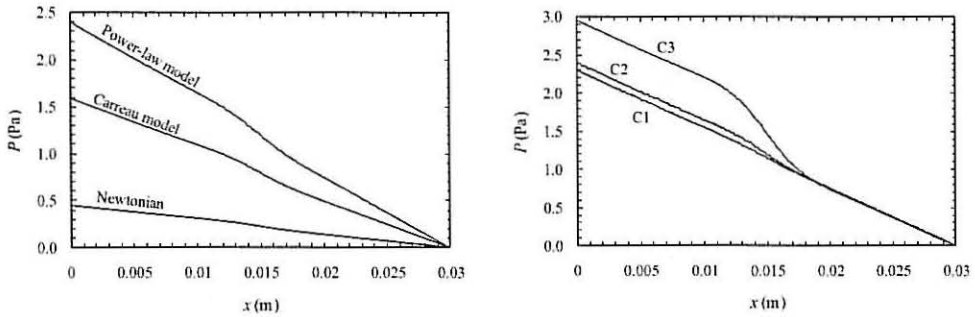

Figure 9: Pressure along Line 1 (Fig. 1). (a) Channel C2 and distinct rheological models. (b) Power-law model and distinct channels.

4. Concluding Remarks

In the present work, the influence of rheological properties of blood and stenosis degree in the properties of the laminar blood flow in stenosed channels has been studied using the commercial finite element code POLYFLOW®. The governative equations were solved using different constitutive models – Newtonian fluid, power-law model and Carreau model. Additionally, different computational domains were also analysed.

The impact of the different rheological models in the velocity profiles were analysed and it was observed that velocities obtained for the Newtonain fluid were slightly different from the ones predicted when the blood was considered a non-Newtonian fluid, this tendency being also observed for the shear rate. Concerning the pressure profiles, different results were obtained for the distinct constitutive equations.

The analysis of pressure and shear rate developed in the wall of the channels shown that he maximum shear rates were achieved in the top of the atheroma and pressure reaches a maximum in the wall of the atheroma.

 ISBN: 978-84-614-6167-7

When the walls of the atheromas are submitted to large pressures, it is possible to generate an endothelium disruption and consequently lead to the formation of a new thrombus. The numerical results revealed that pressure achieves a maximum in the walls of the atheromas, fact that can explain the referred clinical problem.

5. Acknowledgements

The authors acknowledge the financial support provided by: PTDC/SAU-BEB/108728/2008 and PTDC/SAU-BEB/105650/2008 from the FCT (Science and Technology Foundation) and COMPETE, Portugal.

6. References

[1] S.L. ROBBINS, R.S. COTRAN, V. KUMAR, T. COLLINS, *Fundamentos de Robbins – Patologia estrutural e functional*, Rio de Janeiro, 2000.

[2] B.M. JOHNSTON, P.R. JOHNSTON, S. CORNEY, D. KILPATRICK, *Non-Newtonian blood flow in human right coronary arteries: steady state simulations*, J Biomech **37** (2004) 709-720.

[3] H.M. METWALLY, R.M. MANGLICK, *Enhanced heat transfer due to curvature-induced lateral vortices in laminar flows in sinusoidal corrugated-plate channels*, IntJHeatMassTransf **47** (2004) 2283-2292.

[4] C.S. FERNANDES, R.P. DIAS, J.M. NÓBREGA, J.M. MAIA, *Laminar flow in chevron-type plate heat exchangers: CFD analysis of tortuosity, shape factor and friction factor*, ChemEngProc **46** (2007) 825-833.

[5] R.P. DIAS, C.S. FERNANDES, J.A. TEIXEIRA, M. MOTA, A. YELSHIN, *Starch analysis using hydrodynamic chromatography with a mixed-bed particle column*, Carbohydrate Polymers **74** (2008) 852-857.

[6] C.S. FERNANDES, R. DIAS, J.M. NÓBREGA, I.M. AFONSO, L.F. MELO, J. M. MAIA, *Simulation of stirred yoghurt processing during cooling in plate heat exchangers*, JFoodEng **76** (2005) 433-439.

[7] C.S. FERNANDES, R.P. DIAS, J.M. NÓBREGA, J.M. MAIA, *Friction factors of power-law fluids in chevron-type plate heat exchangers*, JFoodEng **89** (2008) 441-447.

[8] R. LIMA, C. S. FERNANDES, R. DIAS, T. ISHIKAWA, Y. IMAI, T. YAMAGUCHI, *Microscale flow dynamics of red blood cells in microchannels: an experimental and numerical analysis*, Computational Vision and Medical Image Processing: Recent Trends, Computational Methods in Applied Sciences **19**,Springer, London, 2011.

[9] R. B. BIRD, R. C. ARMSTRONG, O. HASSAGER, *Dynamics of Polymeric Liquids*, John Wiley & Sons, New York, 1987.

[10]F. DELPLACE, J. C. LEULIET, *Generalized Reynolds number for the flow of power law fluids in cylindrical ducts of arbitrary cross-section*, ChemEngJournal **56** (1995) 33-37.

 ISBN: 978-84-614-6167-7